Evaluation of the TOPEX Dual-Frequency Ionosphere Correction

David A. line]

Jet l'repulsion Laboratory

California Institute of Technology

4800 Oak Grow Dr., Pasadena, CA 91109

Telephone: (818) 354-1539

E-mail: imel@daphne.jpl.nasa.gov

Short Title: TOPEX Ionosphere Correction

A *bstract:* I examine the accuracy of the TOPEX ionosphere correction; its depen - dence on ocean and satellite parameters is lcss than 1 cm. The noise in the ionosphere correction is 5 mm rms plus 1 mm pcr meter of significant wave height, which is Letter than the pm-flight measurements. 'l'his correction should be smoothed over a window of 20 seconds in order to achieve minimum noise without sacrificing ionosphere correction precision. ionosphere models must achieve an independent sample spacing of 500 km or lcss in order to allow a sirlglc-frequency altimeter to have an ionosphere correction comparable in accuracy to that of TOPEX.

1. Introduction

The delay of a radar through the ionosphere can be a significant source of error for a satellite altimeter [Stewart, 1985]. The total electron content (TEC) of the ionosphere, i.e. the integrated electron density along a path from a receiver to a satellite, can vary from c1osc to O TECU (1 TECU = 10^{16} e/m^2) to well over 100 TECU, depending upon the time of day, solar conditions, and location [Callahan, 1984]. At the frequency of the Ku-band altimeter this corresponds to range delays of over 20 cm. TOPEX uscs the dispersion of the ionosphere to measure this delay at two different frequencies and correct for it. However, there arc potential difficulties with this "dual-frequency" ionosphere correction: rapid ionosphere fluctuations, dispersion of the radar chirp, higher order frequency-dcpcndcncc of the ionosphere dispersion, frequency-dcpcndcnt altimeter range corrections, range bias between the two altimeters, and altimeter noise in the range determination for each frequency.

Only ionosphere fluctuations on a time scale of the order of the spacing between adjacent Ku- and C-band bursts (i.e. 107 μs, corresponding to a spatial scale of 70 cm)

will contribute in the case of the first item. As we will see in the latter part of this paper, the ionosphere fluctuations on this scale may be safely neglected compared to the other sources of error.

The delay of the radar signal through the ionosphere is a function of frequency and will be slightly different for different parts of the altimeter chirp (linearly ramped frequency with time). For the TOPEX chirp with a 320 MHz bandwidth}], the difference in propagation time at either end of the chirp amounts to 1 % x TECU in cm for Ku-Band and 17% x TECU in cm for C-hand. However, the effect of this "chirp-compression" is symmetric on the radar point-target response. '1'bus, the effect on the ionosphere correction is much less than the propagation time difference listed here.

The ionosphere correction is obtained by assuming a $1/f^2$ frequency-dependence of the range:

$$R_{Ku} = R_0 + a_{Ku}/f_{Ku}^2 + b_{Ku} + c \quad (1)$$

$$R_C = R_0 + a_C/f_C^2 + b_C + c \quad (2)$$

where R_0 is the true range, R_{Ku}, R_C are the ranges measured by the Ku-hand and C-band altimeters, respectively, and a_{Ku}, a_C arc the corresponding ionosphere correction coefficients which arc proportional to the integrated electron density along the radar path. b_{Ku} and b_C represent all of the other frequency-dcpcndcnt corrections such as the electromagnetic bias (EM-Bias). c contains all of the frequency-indcpcndcnt corrections, such as the orbit correction and the tides. Given estimates for b_{Ku} and b_C and assuming a $= a_{Ku} =$ UC (i.e. neglecting effects of higher than sccolld-order frequency dispersion) one may usc measurements of R_{Ku} and R_C to eliminate a in

the above equations and estimate an ionosphere correction:

$$\Delta r_{\text{ion}} \equiv (R_{\text{Ku}} - b_{\text{Ku}}) - (R_0 + c) = \delta_f[(R_{\text{C}} - b_{\text{C}}) - (R_{\text{Ku}} - b_{\text{Ku}})] \tag{3}$$

where

$$\delta_f \equiv \frac{f_{\text{C}}^2}{f_{\text{Ku}}^2 - f_{\text{C}}^2} \tag{4}$$

For TOPEX, δ_f = 0.179. 1 have defined the ionosphere correction as a positive quantity, which is opposite its sense in the merged geophysical data records (MGDR's), but is more convenient here.

The contribution of the higher order frequency-dcpcndcncc is miniscule. Bassiri (S. Bassiri, Higher order ionospheric effects on the phase delay of electromagnetic signals, JPL memorandum to 1. P. Yunck, March 1988) has estimated the contribution of the next lowest-order term in (1) and (2) (i.e., having a 1 / f^3 dependence) to be about 0.4 cm of range error for a 1.5 GHz radar propagating through a typical earth magnetic field and a relatively large ionosphere electron content of 100 TECU. This corresponds to about $\sim 2 \times 10^{-5}$ cm x TECU for TOPEX. In fact, this is actually an overestimate, because the higher order terms depend on the component of the magnetic field in the direction of propagation of the signal, so that the contribution only reaches this magnitude at the geomagnetic poles, where the nadir signal is parallel to the earth field. Clearly, the higher-order terms are safely neglected.

The correction applied to the Ku- and C-band ranges is a function of significant wave height. (SWH), off-nadir pointing angle (or attitude) and automatic gain control (AGC) of the spacecraft receiver. (The AGC is a function of the cross-section of the surface, a_o, which is related to the wind-speed at the surface.) The correction is written as a polynomial in these quantities, with coefficients which may be different

for the two different frequency bands. Thus if the corrections are not perfect, a frequency-dependent error will be introduced into the range estimation which will propagate into the ionosphere correction. However, this error will be correlated with SWH, σ_0 or attitude, and can thus be detected.

Note that the ionosphere correction itself is highly correlated with ocean and satellite parameters through its latitudinal dependence. Thus only by taking the difference between the altimeter-rnca.surcd ionosphere and independent ionosphere measurements can we observe a correlation between the error in the dual-frequency ionosphere correction and ocean or satellite parameters. Two sources of ionosphere data are convenient; the DORIS ionosphere correction is provided by the Centre National d'Etudes Spatiales (CNES) on the MGDR's, and the international network of GPS (Global Positioning System) data can be interpreted as measurements of the earth's ionosphere between the ground receivers and the satellites.

It is conceivable that one of the radars could have a range bias with respect to the other. This would propagate as an offset in the ionosphere correction, and can be detected by comparing the ionosphere measured by TOPEX to other sources of ionosphere measurements.

By optimally filtering the wavenumber spectrum of the ionosphere correction, one obtains estimates for the noise in the ionosphere correction as well as for the magnitude of the ionosphere signal itself as a function of length scale. I use this information to set an optimum averaging scale for the dual-frequency ionosphere correction and to estimate the resolution desirable in any ionosphere model to be used with a single-frequency altimeter.

2. Sources of Ionosphere Data

The international network of approximately 39 GPS receivers distributed world-widc reports the positions of a constellation of approximately 23 satellites. (The number of satellites and receivers providing useful data at any onc time fluctuates.) These satellites transmit a dual-frequency (1 .2276 and 1.57542 GHz) radar signal to the ground stations, which record the differential delays as a function, of time. Thus these measurements can be turned into measurements of the ionosphere over the receivers.

For the comparisons reported here, the ionosphere is modeled simplistically as a slab at an altitude of 400 km, the approximate peak of the F-layer. Errors in vertical TEC obtained duc to this approximation have been estimated by Lanyi and Roth [1 988] to be less than 10%. Note that the electron density is significant for altitudes much greater even than the TOPEX/POSEIDON orbit. Thus the nadir integrated electron density measured by GPS satellites should be somewhat larger than that measured by TOPEX. however, this bias between the two ionosphere measurements is expected to be at the most a few percent of the ionosphere correction, The iono-sphere is assumed constant over the period of the fit (24 hours) in the sun-fixed reference frame and is obtained by fitting the slant-TEC measurements located on the ionosphere shell to a set of real spherical harmonics, Also fit arc the unknown L1–L2 timing offsets for each satellite transmitter and ground station receiver. The complete fit function j is:

$$f(\mathbf{x}) = \sum_{l=0}^{L_{\max}} \sum_{m=0}^{l} a_{lm} Y_l^m(x_5, x_6)/\sin\alpha' + 2.85\frac{\text{TECU}}{\text{ns}}(\Delta t_{x_1} + \delta t_{x_2}) \qquad (5)$$

where

$$\cos \alpha' = \frac{\cos x_3}{x_4} \tag{6}$$

x is a vector with the following components:

$$\mathbf{x} = \begin{vmatrix} x_1 = \text{satellite index} \\ x_2 = \text{receiver index} \\ x_3 = \text{elevation angle measured at ground} \\ x_4 = 1 + \text{Shell height/earth radius} \\ x_5 = \text{geomagnetic colatitude} \\ x_6 = \text{longitude with respect to the sun} \end{vmatrix} \tag{7}$$

and the parameters to be fit are: a_{lm}, the spherical harmonic coefficients, Δt_i, the satellite timing delays, and δt_j, the receiver timing delays.

L_{max} is the maximum order of the spherical harmonic used in the fit. For the comparisons in this paper $L_{max} = 20$, so that one expects to resolve features only at wavelength scales of 1000-2000 km and larger. The geomagnetic latitude refers to the difference in latitude between the observation point on the ionosphere shell and the latitude of the geomagnetic equator. Thus for these maps the ionosphere is assumed only to vary with geomagnetic latitude and local time. The technique used here is very similar to that of Wilson, *et al.* [1 993].

A typical fit using singular value decomposition to a full day of GPS data is shown in Figure 1. The global rms of the residuals to the fit, corrected for elevation angle to convert to nadir TEC, is about 10 TECU, or about 2 cm in terms of range delay at Ku-band. Fitting to data acquired over shorter time intervals than 24 hours has been explored. The fit residuals then correspond to a nadir range delay of less than I,0 cm rms. However, the coverage is much worse, and the uncertainty in the

comparison to the TOPEX ionosphere correction suffers unacceptably. In addition to the GPS-derived ionosphere correction, wc usc the DORIS ionosphere correction [Picot and Escudier, 1994] provided by CNES on the MGDR's as a independent source of ionosphere data.

Since the sun's position is the dominant effect on electron density, one wishes to sample the ionosphere at different times of the day. In order to accomplish this, it is convenient to select a sequential set of six cycles of MGDR's. During this period, the nearly sun-synchronous TOPEX/POSEIDON orbit passes through approximately onc half of a day of local time. The ascending and descending passes sample local times about onc half of a day apart, so that a six-cycle sequence yields an entire day of local time data. Here, 1 have selected cycles 13-18. Only data for which the Iono_Bad and Geo_Bad_1 flags were clear and for which the Iono_Dor_Bad index was less than 5 have been used.

Several passes from cycle 18 arc shown in Figure 2. They display the extent to which the GPS- and DORIS-derived ionosphere corrections and that of TOPEX agree. Notice especially that the agreement between the GPS-derived correction and that of TOPEX is poor below about 35 degrees southern latitude. This is due to the lack of coverage of GPS receivers in that region, which causes the fit to be poorly constrained there, Because of this, the comparisons in sections 3-5 have been restricted to the region above 35 degrees southern latitude.

Histograms of the three ionosphere corrections are shown in Figure 3, Several things are apparent in this figure: the TOPEX ionosphere correction after smoothing over a 21 second window to reduce the noise contains no values less than --1 cm, and seems consistent with the minimum ionosphere correction being O cm. Both the

DORIS and the GPS ionosphere corrections show superficial 'zeroing" of data. In the case of the GPS correction, this occurred where the fits predicted a negative value for the integrated electron density, always in the southern hemisphere where the fit was poorly constrained. The GPS data also show much larger values than either the DORIS or the TOPEX data, and the DORIS correction histogram shows the effect of quantization.

Figure 4 illustrates that the primary dependence of the ionosphere electron density is on the sun's position. In this figure, the mean TOPEX ionosphere correction as well as the mean difference between TOPEX and GPS and also TOPEX and DORIS have been binned versus local time. The data for this figure were restricted to the equatorial region, which has by far the greatest variability y in vertical integrated electron density. Evidently there is a 1 cm offset between the TOPEX and DORIS ionosphere corrections. The lack of spatial resolution in the GPS-derived correction introduces large errors which are also apparent in this figure.

3. Correlation to Ocean and Satellite Parameters

The difference between the dual-frequency ionosphere correction and GPS is plotted as a function of SWH, attitude, σ_0 and latitude in Figure 5, and for the DORIS ionosphere model in Figure 6. The difference between the TOPEX correction and the DORIS and GPS corrections, respectively, is plotted versus the TOPEX ionosphere correction itself in Figs. 7a and b. These plots represent averages over cycles 13-18. The error bars plotted in Figs. 5-7 correspond to the standard error for each bin, i.e. the standard deviation of the distribution of values for each bin divided by the square root of the number of data in the bin. For most of the data, these error bars

arc much smaller than the plot symbol. With the exception of the latitudinal profile, the differences vary only by about ±0.5 cm across the occupied parameter space. The latitudinal profile has excursions about twice that magnitude, perhaps indicating the influence of the equatorial anomaly (for example, see pp. 192ff of [Kelley, 1989]). Figure 7 again indicates both that the difference between the DORIS and TOPEX ionosphere correction can be characterized by a constant offset of approximately 1 cm and that the poor spatial resolution of the $L_{max} = 20$ spherical harmonic fit to the GPS data is limiting its ability to resolve localized ionosphere features.

Plots such as Figs. 5-7 were made for each cycle separated by ascending and descending passes, and the binned ionosphere correction difference was fit, weighted by the standard errors of each bin, to a straight line function of the independent variable. The standard deviation of the fitted slopes for each group of passes may be used as an estimate for the uncertainty in the fit to the entire data set. These results are summarized in Table 1. I conclude that the dependence of the dual-frequency ionosphere correction on ocean and satellite parameters is less than ±0.5 cm for over 99% of the data and is consistent with zero.

One may also place a bound on the error in the difference between the Ku- and C-band EM-Bias correction, averaged over windspeed. The EM-Hiss correction is parametrized as a percentage of SWH. Since the SWH-dependence of the ionosphere correction error is less than ±0.5 cm over a range of 10 m of SWH, the error in the difference between the Ku- and C-band EM-Bias parameter must be less than 0.3%.

4. Ionosphere Correction Noise

By employing range measurements from a second altimeter to obtain an ionosphere

correction, one increases the noise of the range estimate over that of a single-frequency altimeter. The range estimate is given in terms of the two range measurements by solving (1) and (2) for R_0:

$$R_0 = (1 + \delta_f)(R_{Ku} - b_{Ku}) - \delta_f(R_C - b_C) - c \tag{8}$$

One may propagate the error in R_0 from the errors in the individual terms of (8) and subtract the contributions due to all other sources of error (Ku-band altimeter noise, other frequency- dependent correction estimates, and frequency-indcpcn dent corrections) to obtain the noise contributed to the range estimate by the dual-frequency ionosphere correct ion:

$$(\Delta R_{ion})^2 = [(1+\delta_f)^2 - 1](\Delta R_{Ku})^2 + \delta_f^2(\Delta R_C)^2 \tag{9}$$

where ΔR_{Ku} and ΔR_C arc the noise errors of the two altimeter frequencies. The altimeter noise was measured in thermal vacuum at the Wallops flight facility, and the results as a function of significant wave height (SWH) arc given in 'Table 2.

In order to estimate the uncertainty in the measurement of the ionosphere total electron content, one first notes that in (1) and (2) the residual frequency-dcpcndcllt corrections (for example the frequency-dcpcndcncc of the EM-Bias), b_{Ku} and b_C, arc of order of magnitude 10-3 SWH. This may be compared to $R_C - R_{Ku}$ (1 .'2 cm/TECU) and ΔR_C from Table 2. (I assume Δb is of the same order of magnitude as b.) Clearly, $b_{Ku} - b_C$ is much less than $R_C - R_{Ku}$ and Δb is much less than ARC, so one may ignore these terms. Then, the ionosphere correction coefficient a is given by:

$$a = \delta_f f_{Ku}^2(R_{Ku} - R_C) \tag{10}$$

so that the uncertainly in the TEC measurement, I, is:

$$\frac{\Delta I}{I} \frac{\Delta a}{a} \left[\left(\frac{\Delta R_{Ku}}{R_C - R_{Ku}} \right)^2 + \left(\frac{\Delta R_C}{R_C - R_{Ku}} \right)^2 \right]^{\frac{1}{2}} \tag{11}$$

Initial data from TOPEX show that these estimates of the noise in the dual-frequency ionosphere correction arc at least approximate] y correct. Figure 8 is a plot of the standard deviation over a 21 second interval of the ionosphere correction versus significant wave-height for cycles 13-18. (Variations in SWH and the ionosphere are small on this scale.) The data lie in approximate agreement with the prediction of the table and arc slightly less noisy. Thus on the average the rms uncertainty in the 1 -second averaged dual-frequency ionosphere correction is about 5 mm plus 1 mm per meter of significant wave height. However, as is shown in the next section, this noise may be reduced substantially without losing accuracy in the ionosphere correction by averaging over several seconds.

5. Wavenumber Spectra

Figure 9a is the along-track power spectrum of the TOPEX, GPS and DORIS ionosphere measurements averaged over cycles 13–1 8. In order to extract the power spectrum of the ionosphere itself, the TOPEX dual-frequency ionosphere power spectrum has been optimally filtered [Press *et al.*, 1992] with the assumption of a power law noise spectrum fitted to the data in the range of 0.13 km^{-1} to 0.35 km^{-1}. The DORIS power spectrum overlies the extracted power spectrum dramatically, while the GPS power spectrum cuts off at wavelengths of about 1000-2000 km, as expected from the number of parameters in the fit. The former implies that the resolving scale of the DORIS ionosphere is sufficient to characterize the ionosphere at the accuracy of TOPEX, while the latter suggests that higher-order fits to GPS data may be de-

sirable. The autocorrelation of the altimeter tracker appears as a decrease in the spectral density in the region of highest wavenumber.

Note the peak in the spectrum of both the filtered TOPEX ionosphere and the DORIS ionosphere. Since it occurs in both data sets, which can be regarded as completely independent measurements of the ionosphere, one expects that it is not simply an artifact of data smoothing or interpolation. The peak does not occur in the GPS spectrum since the wavelength is much smaller than the spectrum cutoff. 'l'he wavelength (about 400 km) and magnitude (about 5 x 10-5 of the spectral density at the largest scales) of this peak correspond well to those of Traveling Ionospheric Disturbances, or TID's [Callahan, 1984].

The integrated spectral density in terms of range delay at Ku-band is plotted in Figure 9b. in order to characterize the spatial variability of the ionosphere, the wavelength at which the integrated spectral density reaches 2 mm rms is tabulated for each cycles' ascending and descending passes separately, each of which is roughly constant in local time. Table 3 lists the local times for each group of passes and gives the maximum independent sample spacing based on the Nyquist criterion of a minimum of two samples per wavelength. Thus an ionosphere model should have an independent sample spacing of at most 500 km in order to achieve the same precision as the TOPEX ionosphere correction at all times of the day. The integrated spectral densities were also computed for the equatorial region alone, 30 degrees S to 30 degrees N latitude, The results were very similar to those shown in Table 3. Experimentally, one finds that an averaging interval of about one-fourth the Nyquist sample spacing avoids any systematic bias between the averaged ionosphere correction and the 1 second averages. This is especially important across the rapidly varying

integrated electron densities of the equatorial anomaly, where longer averaging times can introduce biases of 1 cm or more. One concludes from Table 3 that the TOPEX correction can be safely smoothed with a 20 second window. Figure 8 shows the standard deviation of the ionosphere correction after smoothing over this interval; the noise has been reduced to about 2 mm rms.

6. Conclusion

1 conclude from the agreement with the DORIS and GPS ionosphere data that the TOPEX dual-frequency ionosphere correction is accurate at least to 1 cm, and has a dependence upon satellite and ocean parameters of less than 1 cm. The TOPEX ionosphere correction should be averaged over 20 seconds, which allows the noise in the correction to be reduced to about 2 mm rms without introducing errors for the most rapidly varying regions of the ionosphere. '1'here is an average bias of about 1 cm between the TOPEX ionosphere measurements and the DORIS model, Morris and Gill [1994] uses the variability of lake surface heights measured by the altimeter to compare the accuracy of the DORIS and TOPEX ionosphere corrections. The results of that paper seem to indicate in favor of the dual-frequency ionosphere correction. The GPS-derived ionosphere maps are limited at present by the spatial resolution of the fit function and the poor coverage in the lower southern hemisphere.

In order to utilize a sing]e-frequency altimeter, onc needs a source of ionosphere correction data. Roth GPS maps and the DORIS ionosphere model are candidates, as arc other models such as the PRISM model. (W. S. Schreiner and G. H. Born, Iono-spheric Calibration for Single Frequency Altimeter Measurements, preprint from the Colorado Center for Astrodynamics Research, Department of Aerospace Engineering

Sciences, University of Colorado, Boulder, September 15, 1993.) To be as precise as TOPEX, these maps and models should be based on an independent sample spacing of no more than 500 km.

Acknowledgment

The research described in this paper was carried out by the Jet Propulsion Laboratory, California Institute of Technology, under contract with the National Aeronautics and Space Administration. I would like to thank Ernesto Rodriguez, Victor Zlotnicki, Phil Callahan, Charles Morris, Akiko Hayashi, Lee-Leung Fu and Ed Christensen for their assistance and helpful discussions.

References

Callahan, P. S., Ionosphere Variations Affecting Altimeter Measurements: A Brief Synopsis, Marine Geodesy, 8, pp. 249-263 (1984).

Kelley, M. C., The *Earth's Ionosphere:* Plasma *Physics* and Electrodynamics, 484 pp., Academic Press (San Diego) 1989.

Lanyi, G. E. and T. Roth, A comparison of mapped and measured total ionospheric electron content using global positioning system and beacon satellite observations, *Radio* Science, 23, pp. 483-492 (July- August 1988).

Morris, C. S. and S. K. Gill, Evaluation of the Topex/Poseidon Altimeter System Over the Great Lakes, Journal of *Geophysical* Research, this issue.

Picot, N. and P. Escudier, Altimeter Ionospheric Correction from DORIS, Journal of *Geophysical* Research, this issue.

Press, W. H., S. A. Teukolsky, W. T. Vetterling, and B. P. Flannery, *Numerical* Recipes *in C: The Art of* Scientific Computing, second edition, 994 pp., Cambridge Press (New York) 1992.

Stewart, R. H., Methods of Satellite Oceanography, 360 pp., University of California Press, (Berkeley) 1985.

Wilson, B. D., A. J. Mannucci, and C. D. Edwards, Sub-Daily Northern Hemisphere Ionosphere Maps Using the IGS GPS Network, Proceedings of the *7th International Ionospheric Effects Symposium*, J. Goodman cd., Alexandria VA, May 1993, in press.

Captions

~'able 1. Correlation coefficients and slopes from straight line fits to the difference between the TOPEX dual-frequency ionosphere correction and both the GPS and DORIS ionosphere corrections, In obtaining these results, the following restrictions were placed on the data: SWH less than 12 meters, attitude less than 0.5 degrees, C_{J_0} between 8 dB and 17.5 dB, and latitude north of --35 degrees.

Table 2. The pre-flight measurements of the altimeter noise and the corresponding contribution of the ionosphere correction to the random range error. Also, the corresponding uncertainty in the dual-frequency measurement of the total-electron content of the ionosphere (A I). These values are for 1 second averages. The data in the last column may be directly compared to Figure 8. (These data were obtained from the NASA TOPEX Altimeter Consent-to-Ship Package, NASA/GSFC/Wallops night Facility, APL, 5 June 1991.)

Table 3. The Nyquist sampling interval to achieve an ionosphere error of 2 mm rms or less is tabulated as a function of the average local time of the passes from which this interval was computed. For a given cycle, "A" refers to the ascending passes and "D" the descending passes. The "safe" averaging time corresponding to each sampling interval is also tabulated.

Fig. 1. Spherical harmonic fit to GPS data for March 17, 1993. The values of the contour arc in TECU. (4.6 TECU equals 1 cm of range delay at the Ku-band altimeter.) The electron density is largest when the sun is overhead and at all local times along the geomagnetic equator. The 1000–2000 km wavelength resolution of the fit is apparent in the figure.

Fig. 2. Several sample passes from cycle 18. The scattered points are the TOPEX dual-frequency ionosphere correction. For comparison, the corresponding ionosphere corrections from DORIS (thin line) and the GPS maps (thicker line) arc plotted. The paucity of coverage for the GPS data in the southern hemisphere is apparent in that the fits arc poorly constrained in that region.

Fig. 3. Histogram of the TOPEX dual frequency ionosphere correction, the DORIS ionosphere correction and the ionosphere correction derived from spherical harmonic fits to GPS data. These histograms were accumulated over cycles 13-18. The TOPEX ionosphere correction has been smoothed over a 21 second window.

, Fig. 4. Local-time dependence of the mean of the TOPEX ionosphere correction for cycles 13–1 8. Also binned is the local-time dependence of the difference between the TOPEX and GPS-derived corrections and also the TOPEX/DORIS difference.

Fig. 5. Correlation of the difference between the TOPEX dual-frequency ionosphere correction and that derived from ionosphere maps produced by fitting to GPS data. These correlations were binned for all passes of cycles 13-18. The difference is plotted versus (a) SWH, (b) attitude, (c) σ_0 and (d) latitude. A positive bias in this figure and Figures 6 and 7 implies that TOPEX measures a larger integrated electron density than the ionosphere model or map being compared. The TOPEX data have been smoothed over an 11 second window.

Fig. 6. Same as Figure 6, but the difference plotted is that between the TOPEX ionosphere correction and the DORIS ionosphere correction.

Fig. 7. Difference between the TOPEX dual-frequency ionosphere correction and a reference ionosphere correction, either (a) DORIS or (b) GPS, plotted as a function of the TOPEX correction. The several negative values for the TOPEX correction are expected as a natural result of the altimeter noise.

Fig. 8. Standard deviation of the TOPEX ionosphere correction over a 21 second window binned against SWH for cycles 13-18. The error bars in this plot are not the standard error (i.e. uncertainty of the mean), but rather the standard deviation of the distribution for each SWH bin. The standard deviations for both the 1 second averaged correction and that smoothed over 21 seconds are plotted. The 1 second averages may be compared directly to the pre-flight noise measurements in the last column of Table 2.

Fig. 9. (a) Along-track wavenumber spectrum of the ionosphere as measured by the TOPEX dual-frequency ionosphere correction, the ionosphere correction derived from a spherical harmonic fit to GPS data, and the DORIS ionosphere correction. Also plotted is the spectrum of the TOPEX ionosphere correction after optimal filtering. (b) The integrated spectral density of the ionosphere signal obtained by optimally filtering the TOPEX ionosphere measurement to remove the spectrum of the altimeter noise.

Tables

'l'able 1. Correlation of Ionosphere Correction Differences

Parameter	GPS Corr.	DORIS Corr.	GPS slope	DORIS slope
S WH	–0.012	--0.061	–0.05 ± 0.13 cm/m	--0.07 ± 0.01 cm/m
Att	+-0.053	+ 0.009	+3.9 ± 9.4 cm/deg	+0.2 ± 1.7 cm/deg
σ_0	+0.018	+0.047	-10.04 ± 0.19 cm/dB	+-0.053- 0.01 cm/dB

Table 2. Pre-Flight Altimeter Noise Measurements

S W H	ΔR_C	A	R_{Ku}	ΔR_{ion}	AI
2 m	2.7 cm	1.7 cm	1.2 cm	2,7	TECU
4 m	4.1 cm	2.3 cm	1.6 cm	3.9	TECU
8 m	6.9 cm	3.6 cm	2.6 cm	6.5	TECU

Table 3. ionosphere Variability with Local Time

Local Time	Cycle	Nyquist Sampling Criterion (km)	"Safe" Averaging Time (s)
0120	17A	1000	40
0330	16A	1500	60
0530	15A	1800	75
0720	14A	1900	80
0940	13A	1200	50
1120	181)	670	30
1320	17r)	570	25
1430	16D	510	20
1730	15D	590	25
1920	141)	670	30
2140	13D	630	25
2320	18A	500	20

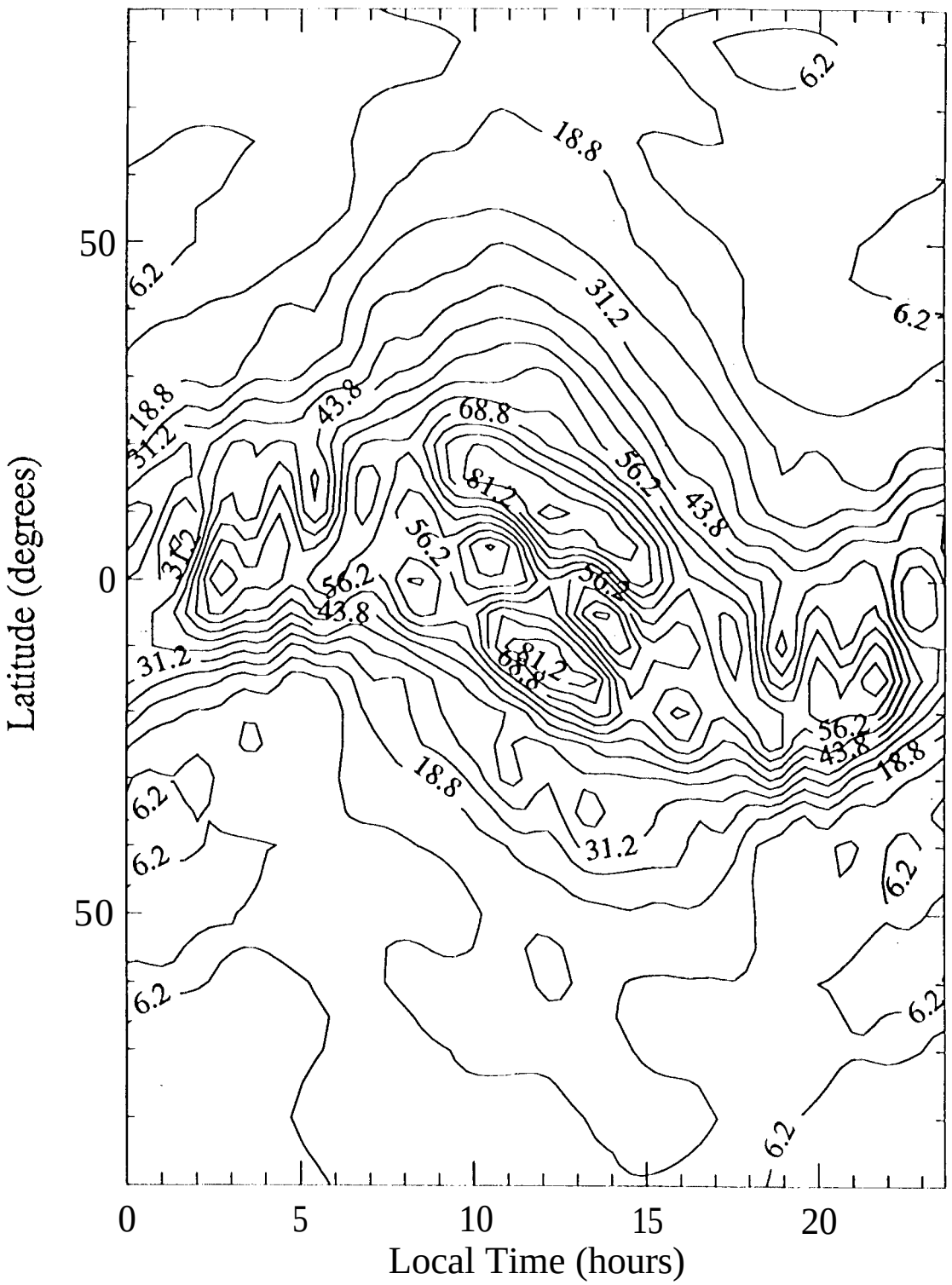
Latitude (degrees)
50
0
50
0
5
10
15
20
Local Time (hours)
6.2
18.8
31.2
43.8
56.2
68.8
81.2

Figure 1

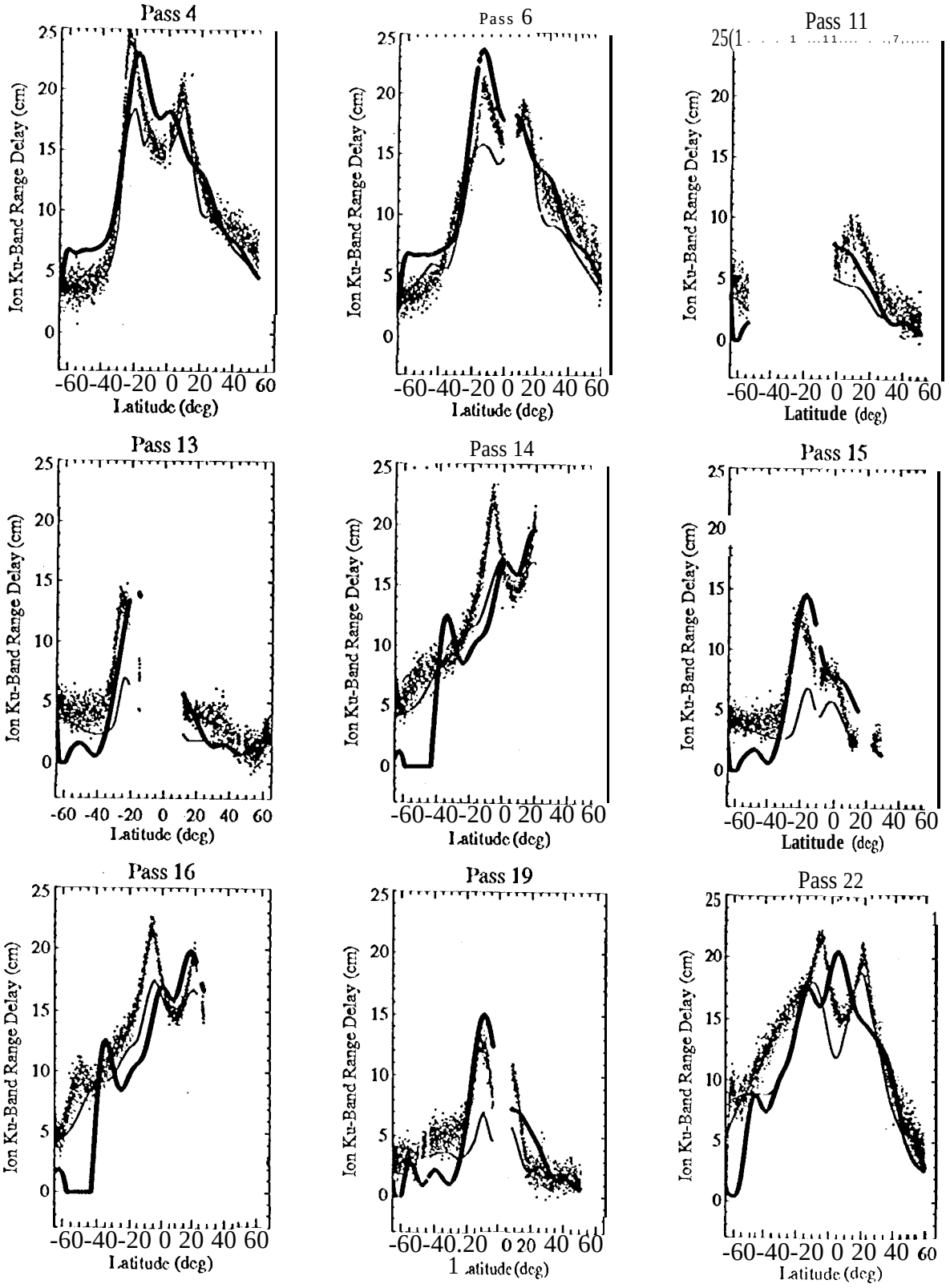
Pass 4
Pass 6
Pass 11
Pass 13
Pass 14
Pass 15
Pass 16
Pass 19
Pass 22
Ion Ku-Band Range Delay (cm)
Latitude (deg)
-60-40-20 0 20 40 60

Figure 2

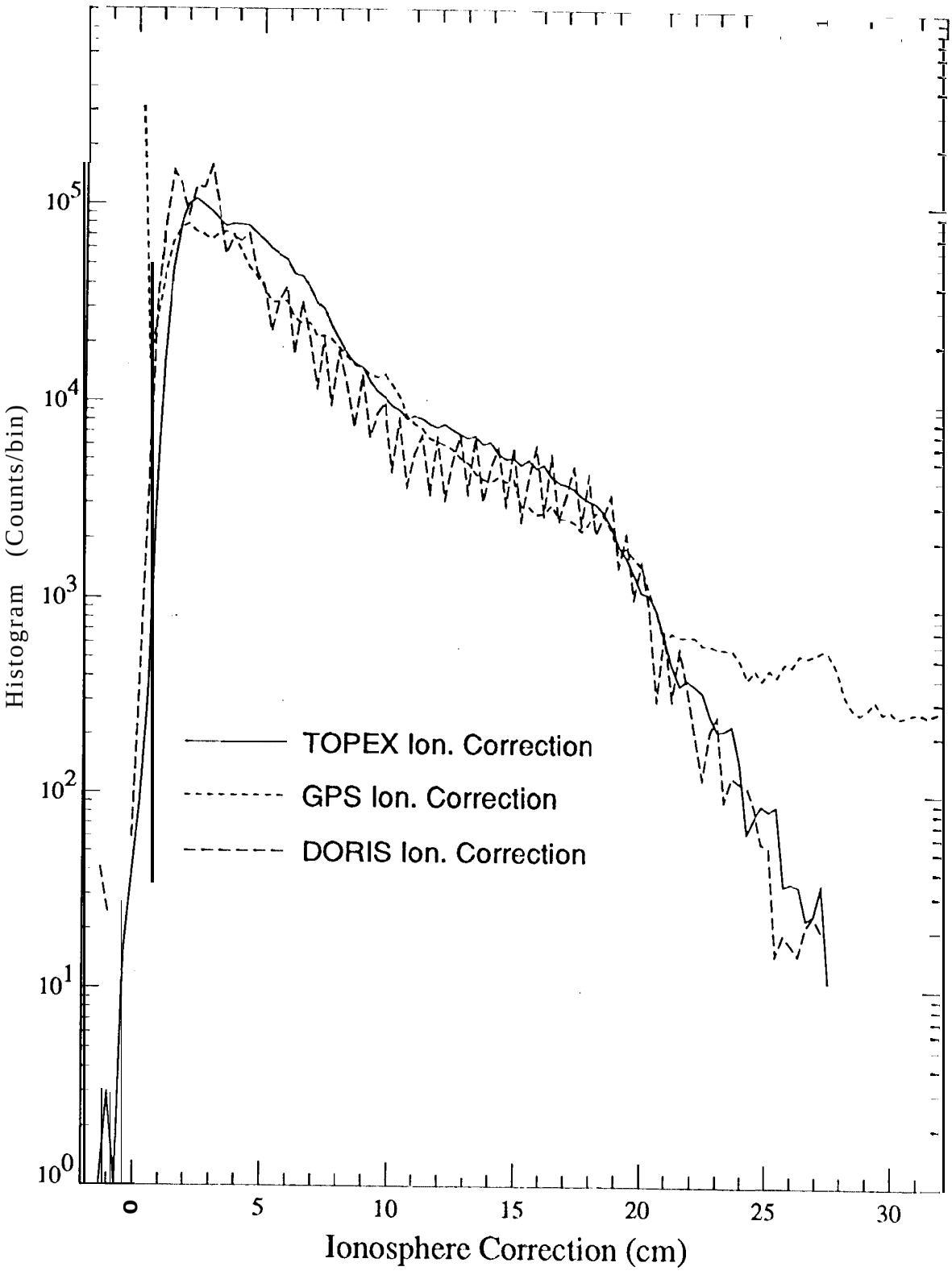
Histogram (Counts/bin)
10^5
10^4
10^3
10^2
10^1
10^0
0
5
10
15
20
25
30
Ionosphere Correction (cm)
TOPEX Ion. Correction
GPS Ion. Correction
DORIS Ion. Correction

Figure 3

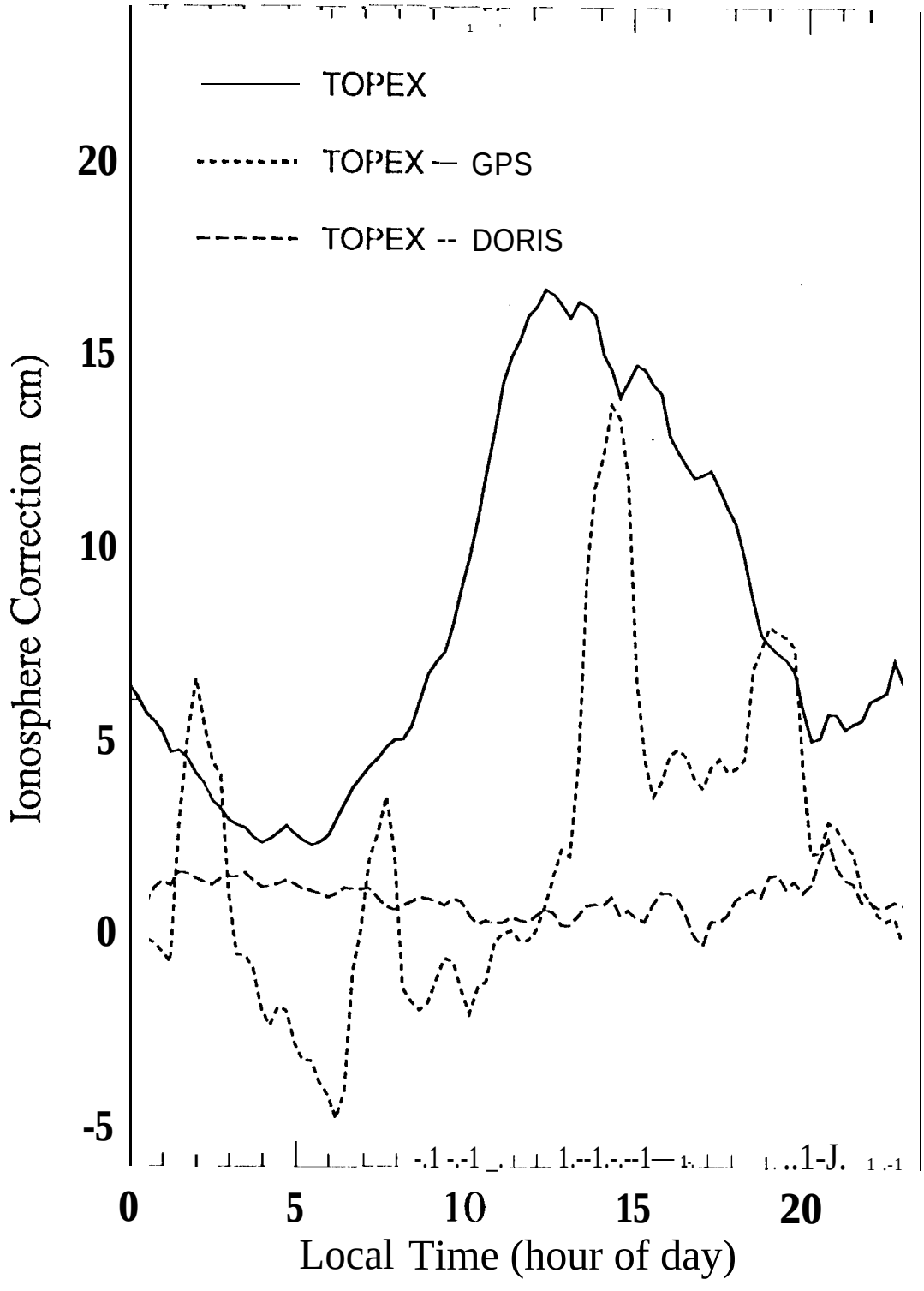
TOPEX
TOPEX — GPS
TOPEX -- DORIS
Ionosphere Correction cm)
20
15
10
5
0
-5
0
5
10
15
20
Local Time (hour of day)

Figure y

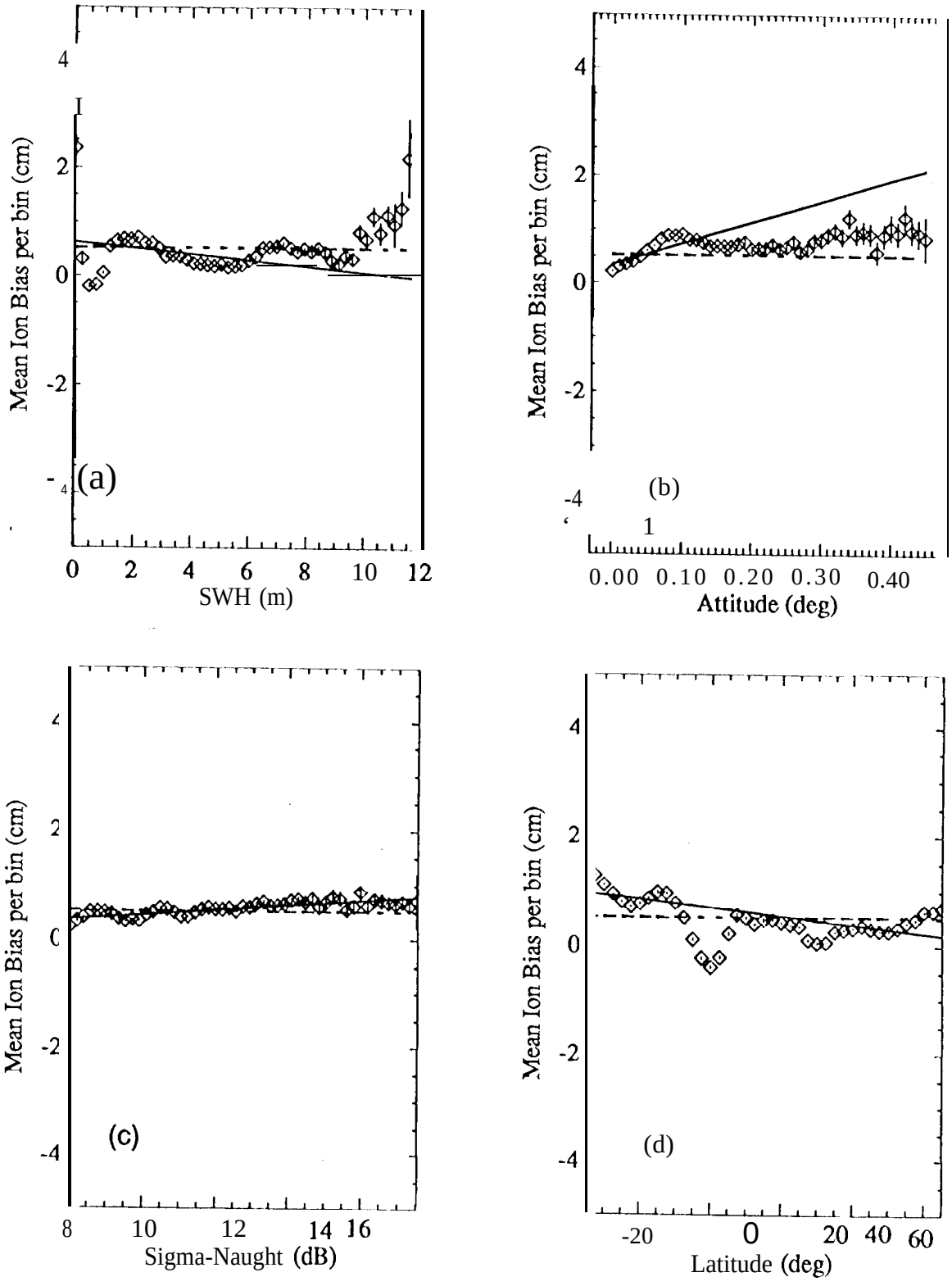
Mean Ion Bias per bin (cm)
SWH (m)
(a)
Attitude (deg)
(b)
Sigma-Naught (dB)
(c)
Latitude (deg)
(d)

Figure 5

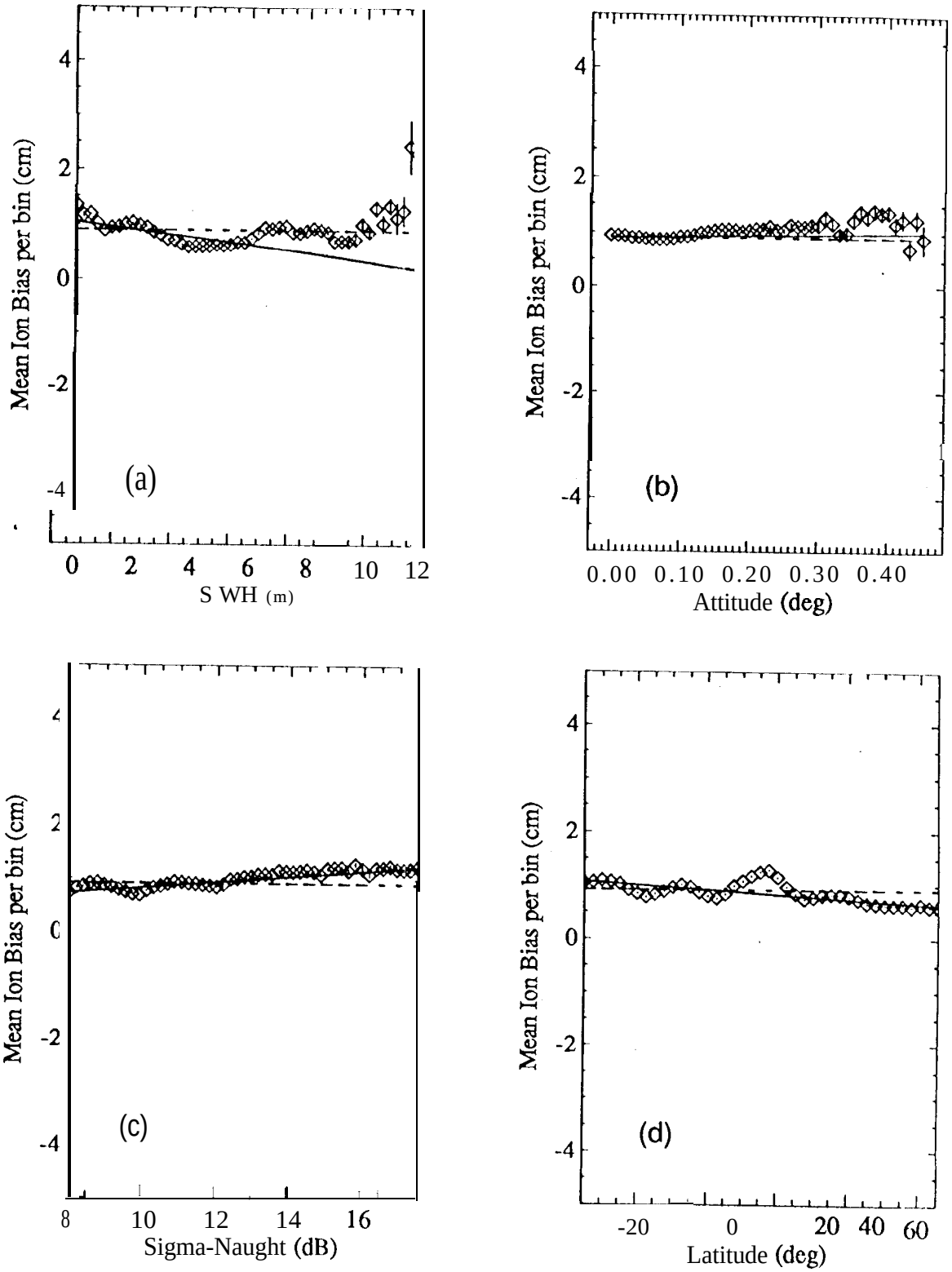
Mean Ion Bias per bin (cm)
4
2
0
-2
-4
(a)
0 2 4 6 8 10 12
S WH (m)
(b)
0.00 0.10 0.20 0.30 0.40
Attitude (deg)
(c)
8 10 12 14 16
Sigma-Naught (dB)
(d)
-20 0 20 40 60
Latitude (deg)

Figure 6

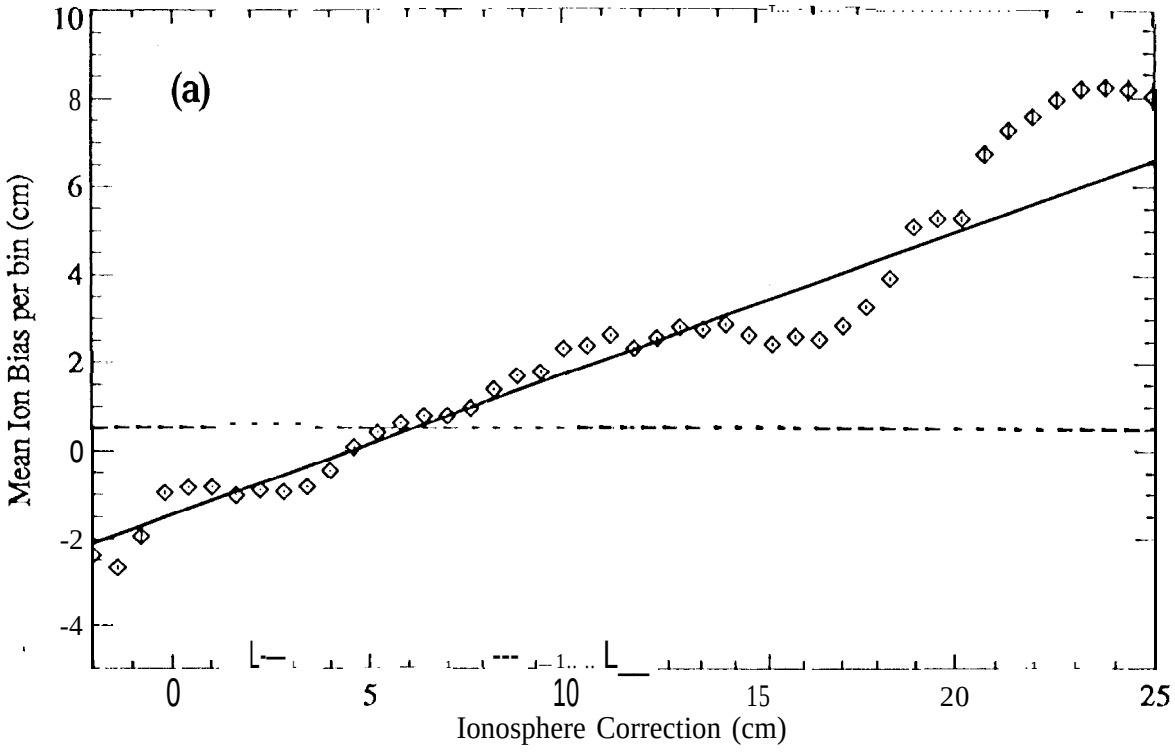
(a)
Mean Ion Bias per bin (cm)
10
8
6
4
2
0
-2
-4
0
5
10
15
20
25
Ionosphere Correction (cm)

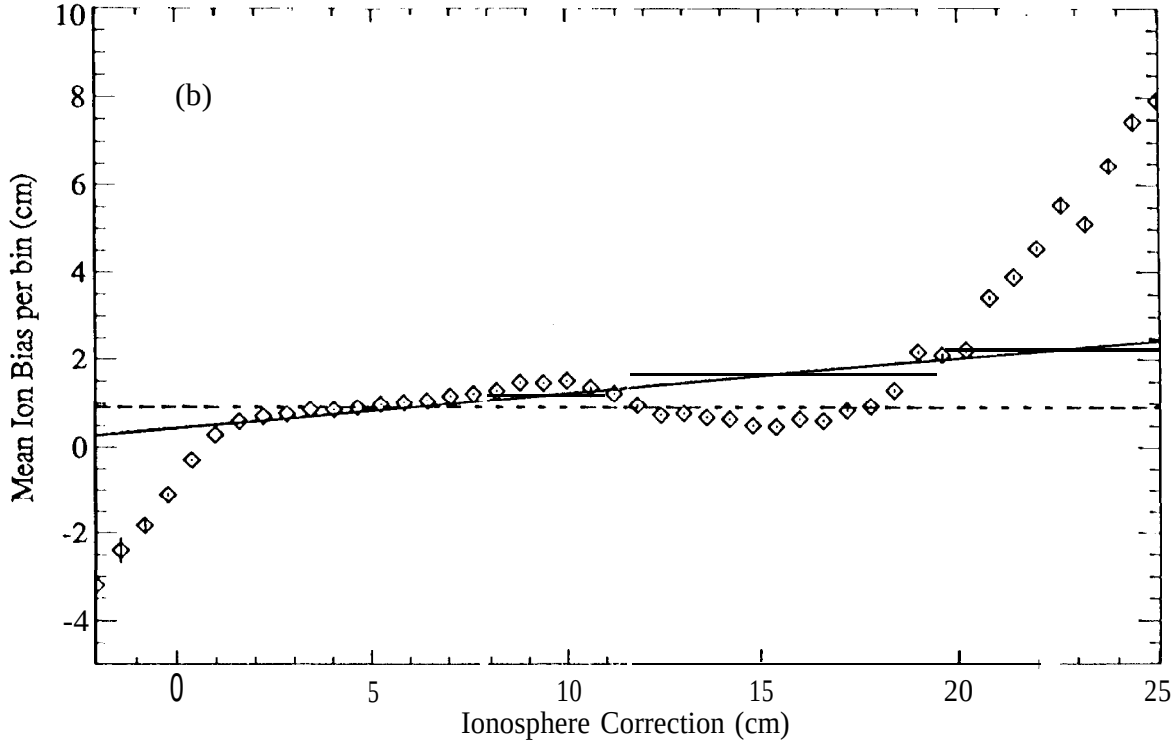
(b)
Mean Ion Bias per bin (cm)
10
8
6
4
2
0
-2
-4
0
5
10
15
20
25
Ionosphere Correction (cm)

Figure 7

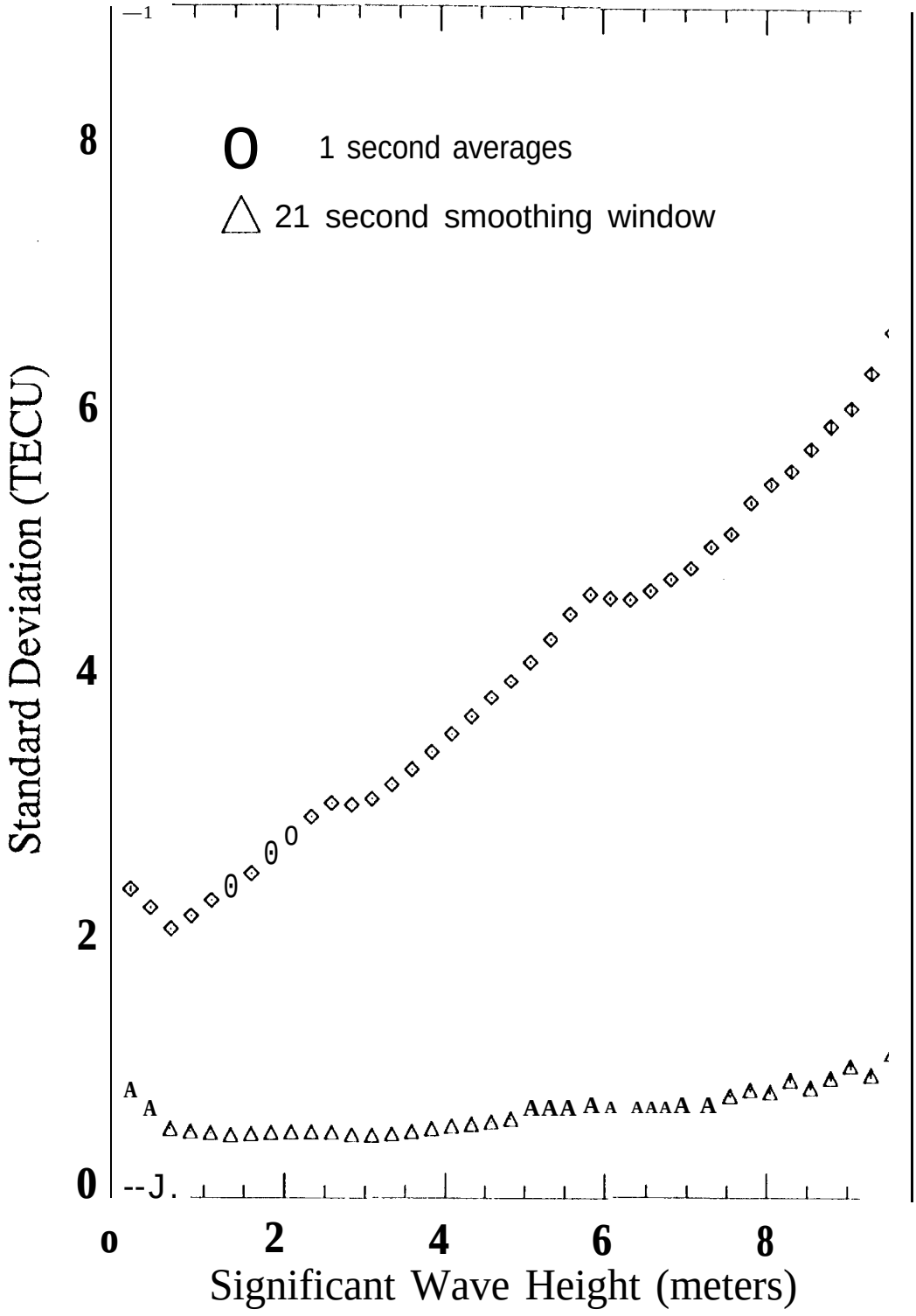
1 second averages
21 second smoothing window
Standard Deviation (TECU)
0
2
4
6
8
Significant Wave Height (meters)

Figure 8

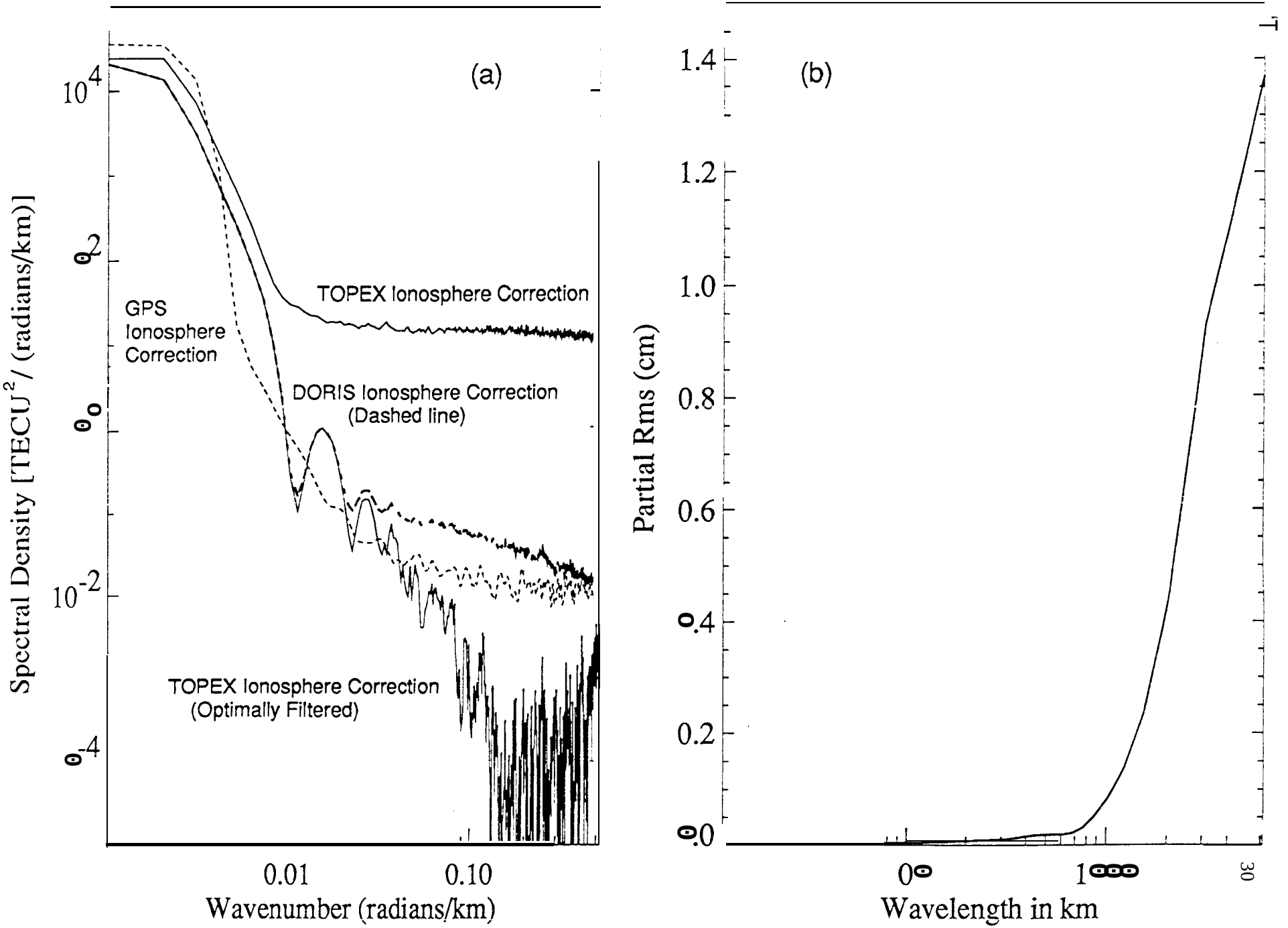
(a)
Spectral Density [TECU^2 / (radians/km)]
10^4
10^2
10^0
10^{-2}
10^{-4}
GPS Ionosphere Correction
TOPEX Ionosphere Correction
DORIS Ionosphere Correction (Dashed line)
TOPEX Ionosphere Correction (Optimally Filtered)
0.01
0.10
Wavenumber (radians/km)
(b)
Partial Rms (cm)
1.4
1.2
1.0
0.8
0.6
0.4
0.2
0.0
0
1000
30
Wavelength in km

Figure 6